⊙ 研究論文

An Analysis of Fully Developed Turbulent Heat Transfer and Flow in an Annulus with the Square-Ribbed Roughness on Both Walls

S. W. Ahn*

양측벽면에 사각돌출형 거칠기가 있는 이중관내의 난류유동과 열전달 해석

안 수 환

Key words : Turbulent Flow (난류 유동), Heat Transfer (열전달), Concentric Annuli (이중동심관), Square - Ribbed Surface Roughness Effect (사각돌출형 표면조도효과).

요 약

양벽면 모두 사각돌출형조도요소가 설치된 동심 이중관내에서 생기는 비대칭 난류유동과 열 전달 특성을, 열전달과 마찰계수에 미치는 조도의 합성효과를 조사하기위해, 연구하였다. 이론해석에서는 한쪽면에 거칠기가 있는 평행평판의 유동에 대한 수정 플란틀 혼합길이(mixing length)이론의 난류모델을 속도분포와 마찰계수를 구하는데 사용하였다. 최대속도지점에서 안쪽과 바깥쪽의 두 속도형상들은 힘의 평형에 의해 일치 시켰다. 그리고나서, 온도 분포와 열전달 계수를 계산하였다. 속도형성과 마찰계수들의 해석 결과는 실험과 매우 잘 일치하였다. 마찰계수와 Nusselt number에 미치는 조도비, 조도에 대한 피치비, 그리고 반경비등과 같은 여러 변수들의 효과들을 조사하였다. 본 연구는 일정의 조도 요소들이 전체적 효율 측면에서 볼때 유리하게 열전달을 향상시킨다는 것을 증명하였다.

Nomenclature(see also Fig. 1)

a thermal diffusivity
C constant, 5.52
c specific heat
K von Karman' s constant
P pitch between roughness elements
Pr_t turbulent Prandtl number
r, R radius
q heat flux
R_j^+ $R_j(\tau_{R_o}/\rho)^{0.5}/\upsilon$
S $R_o - R_i$

* 정회원, 통영수산전문대학

T_j^+ $(T_{Ri} - T_j)C\tau_{Ro}/[q_{Ro}(\tau/\rho)^{0.5}]$
U_j^+ $U_j/(\tau_{Ro}/\rho)^{0.5}$
y distance
y_j^+ $y_j(\tau/\rho)^{0.5}/\upsilon$
Z_{Rj} imaginary location where $U_j=0$
α radius ratio, R_i/R_o
α_{mo} R_m/R_o
δ_j $|R_m - R_j|$
Δ δ_j^+/R_j^+
ε eddy diffusivity
ε roughness height
l mixing length
ξ_j y_j^+/δ_j^+
υ kinematic viscosity
ρ density
τ shear stress

Subscripts :

H Heat
i inner
j i or o
m corresponding to the location of maximum velocity
M momentum
o outer
R radius
r rough
s smooth
t turbulent

1. Introduction

A well-known method to increase the heat transfer from a surface is to roughen the surface either randomly with a sand grain or by use of regular geometric roughness elements on the surface. However, since the increase in heat transfer is accompanied by an increase in the resistance to fluid flow, the heat transfer per unit pumping power expended may not be improved. Therefore, it is desirable to obtain optimum or advantageous geometrical shapes and arrangements of the surface roughness elements.

Lee(1) has shown that certain artificial roughness elements can be used to enhance heat transfer rates with advantages from th overall efficiency point of view. The patterns and effects of surface roughness on turbulent flow can not effectively described by any single parameter, such as the average roughness height, ε. Nevertheless, many studies proceeded as if ε alone were sufficient to describe the flow induced by the surface roughness. Schlichting (2) introduced the concept of equivalent sand grain roughness, Ks, as means of characterizing different types of surface roughness by referring to the equivalent net effect produced by Nikuradse's experiments, which were carried out in pipes that were artificially roughened with uniform grains of sand. Allan & Sharma (3) and Musker & Lewkowicz (4) also attempted to set up models of turbulent flow over rough surfaces.

Unfortunately, all these models require a prior knowledge of the function to describe a particular set of shapes and arragements of surface roughness elements. For such cases, there seems to be no reliable prediction for momentum and heat transfer available in the literature. In our previous report (5) a different approach from these models was used to indirectly describe a particular surface roughness for the prediction pressure loss and heat transfer rate in an asymmetric flow induced by the given roughness elements. This approach was taken because, with asymmetric boundaries, the flow exhibits some characteristic aspects by virtue of symmetry that have been hidden.

In this study, it is assumed that the surface roughness affects only locally on the velocity

profiles and therefore an empirical roughnes correlation previously obtained for the flow between two parallel plates with square – ribbed surface roughness elements on the one surface only (1) could be used in the analysis. This assumption is tested and proved to be realistic (5). The resultant effect of artificial roughness is determined from a comparison of rough and smooth surface with regard to the heat transfer increase relative to the increase in pressure losses.

2. Analysis

Since the energy equation is linear and homogeneous, superposition models are used to obtain solutions for the inner wall heated with the outer insulated.

2. 1 Assumptions(see Fig. 1).

(i) The annulus is concentric. Both the outer wall and the inner core surface are "square – ribbed".

(ii) Velocity and temperature fields in the annulus are fully developed.

(iii) The line of the maximum velocity coincides with the line of the zero shear stress.

(iv) For the rough wall regions, a modified logarithmic velocity profile is used. The surface roughness affects only locally on the velocity profiles.

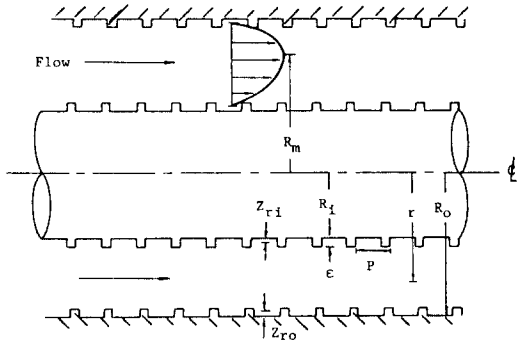

Fig. 1 Idealized Model

2. 2 Velocity and Temperature Distributions

For the velocity and temperature distributions, use is made of the concept of eddy diffusivity, ε_M, and the turbulent Prandtl number, Pr_t. The basic equations governing the transport of momentum and heat can thus be written as :

$$\frac{\tau_j}{\rho} = (\nu + \varepsilon_M)\frac{\partial U_j}{\partial y} \tag{1}$$

$$\frac{q}{c\rho} = (a + \varepsilon_H)\frac{\partial T}{\partial r} \tag{2}$$

For the velocity profiles, we use the following which proved to be reasonable (5) :

$$U_j^+(\xi_j) = \frac{1}{K_j} ln[\xi_j / (Z_{rj}^+ / \delta_j^+)] \qquad (Z_{rj}^+ / \delta_j^+) \le \xi_j \le 1 \tag{3}$$

$$Z_{rj} = y_{mr}\,\mathrm{EXP}\,[(U\tau_{Ro}/U\tau_{Ri}) \{ln(S - y_{mr})(U\tau_{Ro}/\nu) + C\,K_o\}] \tag{4}$$

and from Ref. (5), we obtains :

$$y_{mr} = 0.299 S \mathrm{Re}^{0.066}(S/\varepsilon)^{0.140}(P/S)^{0.201} \tag{5}$$

The term, $(U\tau_{Ri})/(U\tau_{Ro})$, must be obtained from the case of annular flow where an inner core has the roughness elements and the outer wall is smooth (5). Now, from Eqs. [1] and [2], we obtain(see Appendix) :

$$\frac{\partial T_j^+}{\partial \xi_j} = \pm \frac{\partial U_j^+ \left(1 + \frac{\varepsilon_M}{\nu}\right)_j (q_j / q_{Ri})}{\left(\frac{1}{\mathrm{Pr}} + \frac{1}{\mathrm{Pr}_t}\frac{\varepsilon_M}{\nu}\right)_j (\tau_j / \tau_{Rj})} \tag{6}$$

The shear stress distributions, τ_j/τ_{Rj}, and the heat flux distribution, q_j/q_{Ri}, are obtained from force and energy balances, respectively, as follows :

$$\frac{\tau_i}{\tau_{Ri}} = \frac{(1+\Delta_i Z_{Ri}^+/\delta_i^+)[\alpha_{mo}^2 - \alpha^2(1+\Delta_i\xi_i)^2]}{(1+\Delta_i\xi_i)[\alpha_{mo}^2 - \alpha^2(1+\Delta_i Z_{Ri}^+/\delta_i^+)^2]} \quad (7)$$

$$\frac{\tau_o}{\tau_{Ro}} = \frac{[(1-\Delta_o\xi_o)^2 - \alpha_{mo}^2](1-\Delta_o\xi_o)}{(1-\Delta_o\xi_o)[(1-\Delta_o Z_{Ro}^+/\delta_o^+)^2 - \alpha_{mo}^2]} \quad (8)$$

$$\frac{q_i}{q_{Ri}} = \frac{(1+\Delta_i Z_{Ri}^+/\delta_i^+)[(1-\Delta_o Z_{Ro}^+/\delta_o^+)^2 - \alpha^2(1+\Delta_i\xi_i)^2]}{(1+\Delta_i\xi_i)[(1-\Delta_o Z_{Ro}^+/\delta_o^+)^2 - \alpha^2(1+\Delta_i Z_{Ri}^+/\delta_i^+)^2]} \quad (9)$$

$$\frac{q_o}{q_{Ri}} = \frac{\alpha(1+\Delta_i Z_{Ri}^+/\delta_i^+)[(1+\Delta_o Z_{Ro}^+/\delta_o^+)^2 - (1-\Delta_o\xi_o)^2]}{(1-\Delta_o\xi_o)[(1-\Delta_o Z_{Ro}^+/\delta_o^+)^2 - \alpha^2(1+\Delta_i Z_{Ri}^+/\delta_i^+)^2]} \quad (10)$$

2. 3 Eddy Diffusivity for Momentum, ε_M

The eddy diffusivity is defined as :

$$(\varepsilon_M)_j = l_j^2\left|\frac{\partial U_j}{\partial y_j}\right| \quad (11)$$

where $l = K_j(y_j - Z_{rj})$

Eq. (11) can be made dimensionless as :

$$[\varepsilon_M/\nu]_j = K_j\delta_j^+/\xi_j^+[1-(Z_{rj}\delta_j^+/\xi_j)]^2 F(\tau) \quad (12)$$

where for j=i, $F(\tau) = U\tau_{Ri}/U\tau_{Ro}$ and for j=o, $F(\tau)=1$,

2. 4 Reynolds Number, Friction Factor and Nusselt Number.

The definition of Reynolds number is given by :

$$Re = U_b 2(R_o - R_i)/\nu = 2U_b^+(R_o^+ - R_i^+) \quad (13)$$

Eq.(13) in dimensionless parameters is :

$$Re = \left[\frac{4\alpha}{1+\alpha}\right]\left[\delta_i^+\int_{(Z_{Ri}/\delta_i^+)}^1(1+\Delta_i\xi_i)U_i^+ d\xi_i + \frac{1}{\alpha}\delta_o^+\int_{(Z_{Ro}/\delta_i^+)}^1(1-\Delta_o\xi_o)U_o^+(\xi_o)d\xi_o\right] \quad (14)$$

The average value of friction factor is defined as :

$$f = \frac{2\pi(f_i R_i + f_o R_o)}{2\pi(R_i + R_o)} \quad (15)$$

In dimensionless parameters, we have :

$$f = 8\left\{\frac{(1-\alpha)^2\left[1+\frac{\alpha\tau_{Ri}}{\tau_{Ro}}\right]}{(1+\alpha)}\right\}\left(\frac{R_o^+}{Re}\right)^2 \quad (16)$$

The definition of Nusselt number is :

$$Nu = \frac{2h(R_o - R_i)}{k} = 2\left[\frac{1-\alpha}{\alpha}\right]\frac{R_i^+ Pr}{T_b^+} \quad (17)$$

And the dimensionless bulk temperature in dimensionless parameters becomes :

$$T_b^+ = \frac{4}{Re(1+\alpha)}\left[\alpha\delta_i^+\int_{Z_{Ri}^+/\delta_i^+}^1(1+\Delta_i\xi_i)U_i^+T_i^+ d\xi_i + \frac{1}{\alpha}\delta_o^+\int_{(Z_{Ro}^+/\delta_i^+)}^1(1-\Delta_o\xi_o)U_o^+T_o^+ d\xi_o\right] \quad (18)$$

2. 5 Boundary and Matching Conditions

From a force balance, we obtain the shear stress ratio as follow :

$$\frac{\tau_{Ri}}{\tau_{Ro}} = \left(\frac{R_o - Z_{Ro}}{R_i + Z_{Ri}}\right)\left[\frac{R_m^2 - (R_i+Z_{Ri})^2}{(R_o - Z_{Ro})^2 - R_m^2}\right] \quad (19)$$

It is well established that the standard universal velocity is not fully adequate for the inner velocity distribution of concentric annulus (6, 7). Therefore, while a fixed value of 0.4 for K_o is taken, the value of K_i is to be calculated from the appropriate boundary condition. From the continuity of the eddy diffusivity at the location of the maximum velocity($r = R_m$), we may obtain the following relation from equations (3) :

$$K_i = K_o\frac{\delta_o^+}{\delta_i^+}\frac{[1+(Z_{Ro}^+/\delta_o^+)]^2}{[1+(Z_{Ri}^+/\delta_i^+)]^2}\frac{U\tau_{Ro}}{U\tau_{Ri}} \quad (20)$$

From the continuity of velocities at the location of the maximum velocity, at $r=R_m$, $U_{im}= U_{om}$ and from the definition, at $r=R_i+Z_{ri}$ and $R_o - Z_{ro}$, $U_j=0$. The equality of temperature at the location of the maximum velocity, ($r=R_m$), and

$$\frac{\partial T_i}{\partial r} = \frac{\partial T_o}{\partial r} \tag{21}$$

$$\frac{\partial^2 T_i}{\partial r^2} = \frac{\partial^2 T_o}{\partial r^2} \tag{22}$$

The matching conditions (21) and (22) are required because the derivative of temperature profile is locally diverged at the point of the maximum velocity. To obtain the results for a given Reynolds number, first of all, a Reynolds number should be given ; however, the Reynolds number is actually obtained from the velocity profile, and the velocity profile is obtained from the given Reynolds number.

Therefore, a two - dimensional iteration method is used ; one is for the velocity, and the other is for the Reynolds number. For the initial guess, a dimensionless sublayer thickness (ξ_{sub}) is used, and the dimensionless sublayer thickness(ξ_{sub}) is the number between 0 and 1, so that R_o^+ and R_m^+/R_o^+ are the variables of Reynolds number. With the guessed R_m^+/R_o^+, the velocity profiles in the smooth and rough parts are obtained, where we use the 5 - point Gaussian quadrature integration method. At the maximum velocity position, we check the equality of velocity. With the condition that velocities of both parts are equal, the Reynolds number is calculated with the velocity profiles obtained from Simpson' s integration method with the number of nodes equal to 5000. If the velocities are not equal, we reguess the value of R_m^+/R_o^+. If the calculated Reynolds number is equal to the given Reynolds number, the velocity profile is obtained. Finally, the friction factor, temperature profile, bulk temperature, and Nusselt number are calculated. And we use the parameters in calculation as follows :

Table 1 Parameters used in calculation

	class	range
Input parameters	α	0.2, 0.4, 0.5, 0.8 and 0.9
	R_o^+	in terms of R_e : 10^4 to 10^5
	Pr	0.1, 0.72, 1.0, 2, 7 and 30
	P/ε	2, 4 and 8
	S/ε	9.7, 19.4 and 25
	Prt	fixed at one for this paper

3. Results and Discussion

Representative velocity profiles from the analysis are shown in Fig. 2. The previous analytical and experimental study for the case of an annulus which had the same roughness element as those of the present study on the

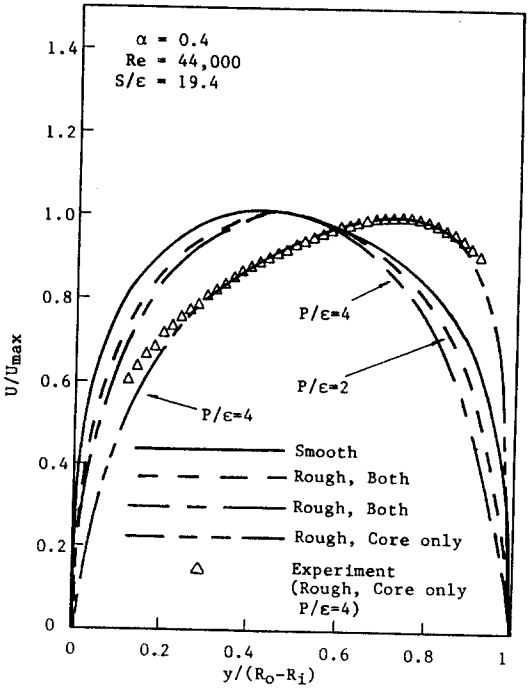

Fig. 2 Velocity distribution

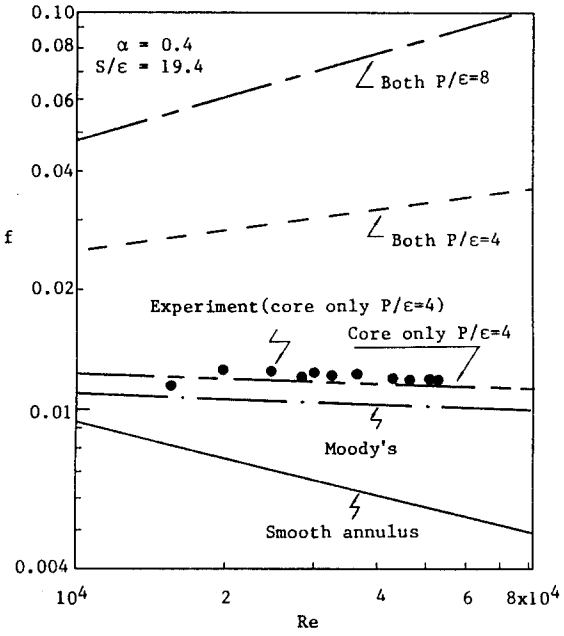

Fig. 3 Friction factor

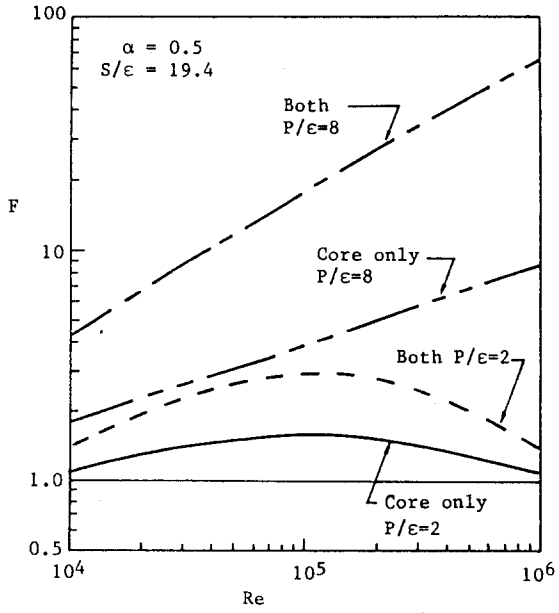

Fig.4 Friction factor ratio. F

core surface only (5) is also shown in the figure as a reference.

The loci of the maximum velocity of the present case where the roughness elements are on both wall surfaces are closer to the core tube. This is expected as the present case is analogous to that of the concentric annuli with smooth wall surfaces. The data for other ranges of parameters showed similar trend. Although we do not have any experimental data, it may be deduced from our previous study (8), the velocity profiles predicted must be very close to the actual measurement.

It is expected that the assumption used in the analysis diverges from the reality with increasing value of P/ε because of Eq. (5). It is obvious from the figure that the friction factor is strongly affected by the roughness density, P/ε. It was also seen that f was also affected by the relative height of roughness, S/ε, as well as by the geometry of roughness elements. The figure also illustrates the deficiency of the Moody's diagram.

In Fig. 4, the increase in pressure losses in terms of friction factor due to the roughness elements on the both wall surfaces is normalized by that of the smooth case. The normalized friction factor is defined as ;

$$F = f_r / f_s \tag{23}$$

The effect of P/ε is significant.

The effect of S/ε on F is also seen but is less and the trend is opposite, that is, F decreases with increasing S/ε for the range of the parameters studied.

Heat transfer in terms of Nu is also normalized as :

$$H = Nu_r / Nu_s \tag{24}$$

The effects of P/ε and Pr on H are seen in Fig. 5 to be similar to the trends observed for the annuli with roughness on the core tube surface only (5). However, the magnitude of the values of H is always higher than that of the latter. The additional roughness on the outer wall must have contributed to the increase in

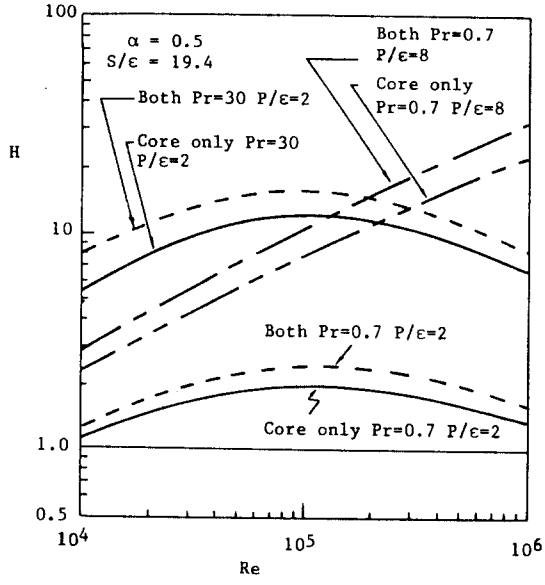

Fig. 5 Heat Transfer Ratio, H

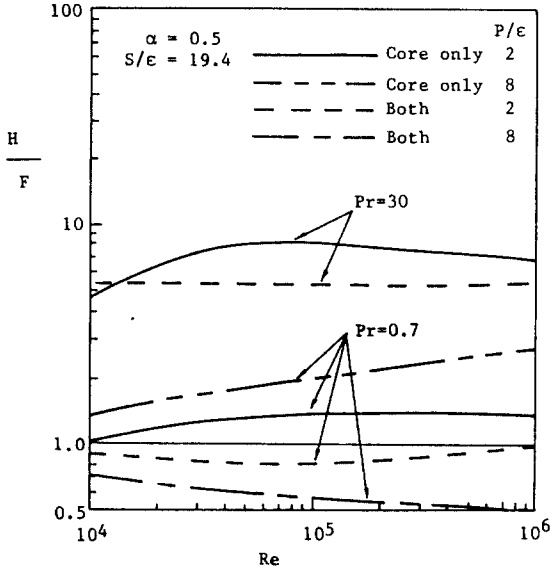

Fig. 6 The effects of P/ε and Pr on H/F

heat trasnfer as was the case of F as seen in Fig. 4. The values of H are seen to be slightly less than those of H for the same conditions.

The resultant effect of artificial roughness is determined from a comparison of rough and smooth surfaces with respect to the heat transfer increase relative to the increase in pressure losses. This is expressed in terms of a non - dimensional parameter, H/F, which is defined as :

$$H/F=(Nu_r/Nu_s)/(f_r/f_s) \qquad (25)$$

(H/F)>1 suggests that the increase in heat transfer due to roughness is greater than the increase in pressure loss due to roughness and therefore it is advantageous to have the particular roughness elements from the overall efficiency point of view.

Fig. 6 shows the effects of P/ε and Pr on H/F for the case of the annuli with roughness on the core only, the ratio H/F is always greater than unity, for Pr=0.7 and 30, implying that the increase in heat transfer due to the presence of the roughness element is greater than the increase in the pressure drop. However, for the present case, the values of H/F for Pr=0.7 are less than unity. This is due to the fact that the presence of the roughness elements on the outer wall increases the pressure drop more than the case where only the core wall has the roughness elements. However, the effect of increasing Prandtl number is to increase the ratio H/F for the

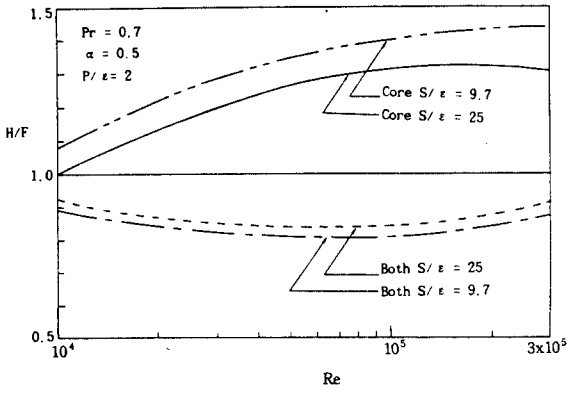

Fig. 7

range of Prandtl number studied.

The effect of Reynolds number on the ratio is seen to be not so simple. H/F decreased with increasing Reynolds number up to about 10. However, a further increase in Reynolds number brings an increase in H/F.

5. Conclusion

The effects of the radius ratio, roughness density, relative roughness height, Reynolds and Prandtl numbers on the parameter H/F are identified for a turbulent flow induced by square-ribbed surface roughness elements on the both walls of a concentric annulus. The study demonstrates that additional presence of roughness elements on the other wall contributes to the increase in pressure drop but certain artificial roughness elements can still be used to enhance heat transfer rates with advantages from the overall efficiency point of view. The required pumping power per unit heat transfer rate decreases with increasing value of P/ε, the decreasing values of S/ε and α, and increasing Prandtl number for the ranges of parameters studied.

Reference

1) Lee, Y., "An Analysis on the Enhanced Heat Transfer induced by Square-Ribbed Surface Roughness", Heat Transfer Sci. and Tech., Hemisphere Pub. Co., N.Y., pp. 781-788, 1987.
2) Schlichting, H., "Boundary Layer Theory", 6th ed., McGraw Hill Book Co., Inc., pp. 578-589, 1968.
3) Allan, W. K. and Sharma, V., "An investigation of Low Turbulent Flows over Rough Surface", Jour. Mech. Eng. Sci., Vol. 16, pp. 71-78, 1974.
4) Musker, A. J. and Lewkowicz, A.K., "The Effect of Ship Hull Roughness on the Development of Turbulent Boundary Layers", Proc. Int. Symposium on Ship Viscous Resistance, SSPA, Goteborg., 1978.
5) Lee, Y. P., Ahn, S. W. and Lee, Y., "Turbulent Fluid Flow and Heat Transfer Induced By Square-Ribbed Surface Roughness in Concentric Annuli", Ninth International Heat Transfer Conference, 4-MC-20, Jerusalem, August 19-24, pp.465-470, 1990.
6) Brighton, J. A. and Jones, J. B., "Fully Developed Turbulent Flow in Annuli", Trans. ASME, J. Bas. Engng., Vol. 86, pp. 835-844, 1964.
7) Jonsson, V. K. and Sparrow, A., "Experiments on Turbulent Flow Phenomena in Eccentric Annular Ducts", J. Fluid Mech., Vol. 25, pp. 65-86., 1965.
8) 안수환, 이윤표, 김경천, "사각돌출형 표면거칠기가 있는 이중동심원관내의 난류유동과 열전달", 대한기계학회논문집, 제17권, 제5호, pp. 1294-1303, 1993.

Appendix

Derivation of Equation (6)

We have to consider two cases of momentum and energy equations ; for j=j and for j=0. Considering the situation for j=i first and dividing equation (2) by equation (1), the temperature gradient is obtained :

$$\frac{\partial T_i}{\partial y_i} = \frac{\partial U_i/\partial y_i (1+\varepsilon_M/\nu) q_i (\rho C)}{\left(\frac{1}{Pr} + \frac{1}{Pr_t}\frac{\varepsilon_M}{\nu}\right)\tau_i/\rho} \qquad (A.1)$$

Using the dimensionless velocity gradient parameter, $\partial U_i/\partial y_i = (\partial U_i^+/\partial \xi_i)(U\tau_{Ro}^2/\upsilon)(1/\delta_i^+)$, and the definition of dimensionless temperature, $\partial T_i/\partial y_i = -(\partial T_i^+/\partial \xi_i)(U\tau_{Ro}^2/\upsilon)(1/\delta_i^+) \times q_{Ri}/C\tau_{Ro}$, and then, substituting these into equation (A.1), we obtain :

$$\frac{\partial T_i^+}{\partial \xi_i} = \frac{\partial U_i^+ \left(1+\frac{\varepsilon_M}{\nu}\right)_i (q_i/q_{Ri})}{\partial \xi_i \left(\frac{1}{Pr} + \frac{1}{Pr_t}\frac{\varepsilon_M}{\nu}\right)_i (\tau_i/\tau_{Ri})} \qquad (A.2)$$

Next, using the same method with that of j=o, we obtain :

$$\frac{\partial T_o^+}{\partial \xi_o} = -\frac{\partial U_o^+ \left(1+\frac{\varepsilon_M}{\nu}\right)_o (q_o/q_{Ri})}{\partial \xi_o \left(\frac{1}{Pr}+\frac{1}{Pr_t}\frac{\varepsilon_M}{\nu}\right)_o (\tau_o/\tau_{Ro})} \qquad (A.3)$$

Adding equation (A.2) to (A.3), the equation (6) is given by :

$$\frac{\partial T_j^+}{\partial \xi_j} = \pm\frac{\partial U_j^+ \left(\frac{\varepsilon_M}{\nu}\right)_j (q_j/q_{Ri})}{\partial \xi_j \left(\frac{1}{Pr}+\frac{1}{Pr_t}\frac{\varepsilon_M}{\nu}\right)_j (\tau_j/\tau_{Rj})} \qquad (A.4)$$